

Excitation of basin modes by ocean-atmosphere coupling

Paola Cessi and Francesco Paparella¹

Scripps Institution of Oceanography – University of California San Diego, La Jolla, CA.

Abstract. A conceptual model of the coupling between the upper-ocean wind-driven circulation and the mid-latitude atmospheric wind-stress illustrates that large-scale basin-wide oscillations with decadal period can be excited. These oceanic modes are also found in the absence of ocean-atmosphere feedback, but they are damped. The period of the oscillation and the spatial structure of the modes are essentially the same with and without coupling. These oscillations are distinct from the coupled modes of variability arising from a delayed negative feedback between the wind-driven flow and the wind-stress. They are ocean-only linear basin modes which become sustained by ocean-atmosphere coupling.

Introduction

Observational [Trenberth and Hurrell, 1994; Nakamura *et al.*, 1997] and modeling studies [Latif, 1998] offer convincing evidence that the mid-latitude ocean and atmosphere have variability on decadal time-scales. In the ocean, these low-frequency fluctuations are expressed in the sea temperature (both surface and subsurface) and in the oceanic mass transport [Curry *et al.*, 1998]. In the atmosphere, the variability in the sea level pressure and associated surface westerlies leads to the migration and focussing of the storm-tracks which funnel weather systems into Europe [Rogers, 1997] and North America [Ting and Wang, 1997].

Several processes have been proposed to explain midlatitude decadal variability. They implicate the oceans to a varying extent and are not mutually exclusive.

A. Low-frequency variability is dominated by atmospheric internal dynamics. Coupling to the ocean merely enhances the low-frequency end of the spectrum by reducing the thermal damping [Battisti *et al.*, 1995].

B. Decadal variability is the result of inherently coupled ocean-atmosphere fluctuations. The original hypothesis of [Bjerknes, 1964] has recently been quantified in several simplified models, e.g. [Jin, 1997] and [Gallego and Cessi, 2000] (hereafter GC00). The essential process is a delayed negative feedback of the oceanic wind-driven flow onto the wind-stress, mediated by the heat balance of the combined atmosphere and upper-ocean system.

C. The intrinsic low-frequency variability of the ocean can force fluctuations in the atmosphere. Sustained variability of the wind-driven circulation has been found by [Berloff and Meacham, 1997].

¹Now at University of Lecce, Lecce, Italy.

Copyright 2001 by the American Geophysical Union.

Paper number 2000GL012660.
0094-8276/01/2000GL012660\$05.00

In the following we discuss a mechanism which belongs to the latter category, i.e. the variability is intrinsic to the oceans. Our model illustrates how certain damped decadal oscillations present in the ocean-only dynamics become sustained through weak coupling to the atmosphere.

The model

Our focus is the upper ocean, whose circulation is dominated by the mechanical forcing exerted by the wind-stress. On decadal time-scales, baroclinic adjustment processes are the most relevant, and their minimal description is provided by the reduced gravity shallow-water equations. With h representing the thermocline depth, the evolution of the system is governed by:

$$\begin{aligned} u_t + uu_x + vu_y - fv &= -g'h_x - ru + \tau/(\rho_1 h) \\ v_t + uv_x + vv_y + fu &= -g'h_y - rv \\ h_t + (hu)_x + (hv)_y &= 0. \end{aligned} \quad (1)$$

The notation is standard: $g' \equiv g(1 - \rho_1/\rho_2)$ is the reduced gravity; $f = f_0 + \beta y$ is the Coriolis parameter. We assume that the only form of friction is interfacial, set by the coefficient r . No-normal flow is enforced on the solid boundaries, located at $x = 0, L$ and $y = 0, L$.

The ocean-atmosphere feedback is modeled after Sura *et al.* [2000] (hereafter S00): the amplitude of the wind-stress is assumed to be proportional to the anomaly of the ther-

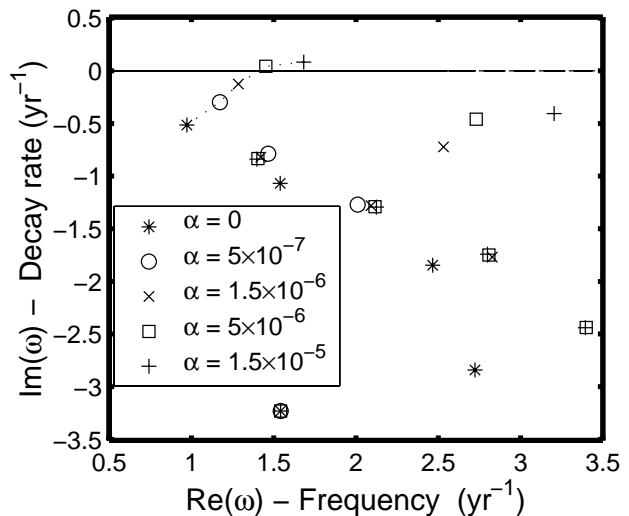


Figure 1. The least damped portion of the eigenspectrum is shown for different values of α (in $m s^{-2}$). The dotted line connects the eigenvalues of the gravest mode. The other parameters are given in Table 1.

mocline depth, h' , averaged over a small sub-basin area, ℓ^2 , whose origin is located at x_o, y_o . Thus

$$\tau = \rho_1 \alpha \cos(\pi y/L) \langle h' \rangle, \quad (2)$$

where

$$\langle h' \rangle \equiv \ell^{-2} \int_{x_o}^{x_o+\ell} dx \int_{y_o}^{y_o+\ell} h' dy. \quad (3)$$

Here h' is defined as the departure of the thermocline depth from the basin-wide average, H :

$$h'(x, y, t) = H - h(x, y, t). \quad (4)$$

The rationale behind the idealized coupling in (2) is that oceanic feedbacks on wind-stress occur due to the wind-driven northward heat transport, proportional to h' . Fluctuations in the oceanic heat transport alter the large-scale atmospheric temperature gradient, which in turn controls the statistics of baroclinic weather systems. The latter are ultimately responsible for the wind-stress in midlatitudes. GC00 show that the oceanic northward heat transport is dominated by the western boundary contribution, and indeed S00 place the coupling area at the western boundary. Moreover, the crucial region for large-scale, midlatitude, air-sea coupling is located at the boundary between the subtropical and subpolar gyre, which coincides with the latitudinal band of maximum oceanic temperature gradients and with the stormtrack. This justifies the choice of placing y_o in (2) at a latitude mid-way through the basin.

An alternative, equivalent coupling procedure has been examined by [Munich *et al.*, 1998]: the amplitude of τ is proportional to h' at a single point. We have examined this representation as well and found that it leads to qualitatively similar results.

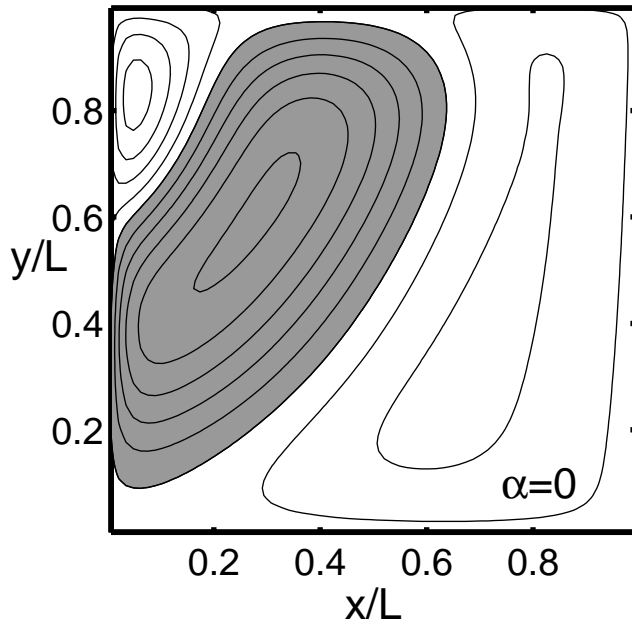


Figure 2. The real part of the eigenfunction associated with the eigenvalue $\omega = 0.97 - i0.52$, denoted by a star with a dotted line in Figure 1.

Table 1. Parameters values

Coriolis parameter	$f_o = 7.4 \times 10^{-5} \text{ s}^{-1}$
β effect	$\beta = 1.6 \times 10^{-11} \text{ m}^{-1} \text{ s}^{-1}$
Mean density	$\rho = 1. \times 10^3 \text{ kg m}^{-3}$
Basin width and length	$L = 3.6 \times 10^6 \text{ m}$
Basin-average depth	$H = 500 \text{ m}$
Reduced gravity	$g' = 0.029 \text{ m s}^{-2}$
Rayleigh friction coefficient	$r = 8 \times 10^{-7} \text{ s}^{-1}$
Latitude of coupling	$x_o = 0 \text{ m}$
Longitude of coupling	$y_o = 1.5 \times 10^6 \text{ m}$
Length of the coupling area	$\ell = 5 \times 10^5 \text{ m}$

Linear analysis

To analyze the emergence of sustained decadal oscillations, we solve the eigenproblem associated with the linearized version of (1). We assume that

$$[u, v, h'](x, y, t) = e^{-i\omega t} [\hat{u}, \hat{v}, \hat{h}](x, y). \quad (5)$$

This leads to the eigensystem:

$$\begin{aligned} -i\omega \hat{u} - f\hat{v} &= -g'\hat{h}_x - r\hat{u} + \alpha \cos(\pi y/L) \langle \hat{h} \rangle / H \\ -i\omega \hat{v} + f\hat{u} &= -g'\hat{h}_y - r\hat{v} \\ -i\omega \hat{h} + H\hat{u}_x + H\hat{v}_y &= 0, \end{aligned} \quad (6)$$

with $\hat{u} = 0$ at $x = 0, L$ and $\hat{v} = 0$ at $y = 0, L$. The eigenvalues ω and the eigenfunctions $[\hat{u}, \hat{v}, \hat{h}]$ are found numerically by using a finite difference approximation of 6. Figure 1 shows the least damped end of the eigenspectrum for five different values of the coupling parameter α . The other parameters have the values listed in Table 1, closely following S00. The dotted line highlights the mode which undergoes a transition from damped to growing as α is increased.

The real part of \hat{h} of the least damped mode for $\alpha = 0$ is contoured in figure 2. The other values of α , not shown here, have a similar structure.

Thus there is an ocean-only oscillatory mode which becomes sustained through the coupling of the wind-driven transport to the wind-stress. It is the gravest, least damped basin mode that occurs in a baroclinic ocean. The period is one transit time, T , of a baroclinic Rossby wave across the basin at $y \approx 0.3L$. The transit time is a strong function of latitude and is given by:

$$T = Lf^2 / (\beta g' H). \quad (7)$$

Other modes, with progressively higher damping rates, have frequencies which are integer multiples of the lowest one. Because of the large-scale interior structure of the modes (as shown in figure 2), the damping rate of the gravest mode is very weak, indeed much weaker than the interfacial dissipation, $r = 14 \text{ days}^{-1}$. Moreover, in the limit $r \ll \beta L$, the decay rate is independent of r [Cessi and Louazel, 2001].

Nonlinear equilibration

We have performed numerical integrations of the complete shallow water equations (1) for several values of the coupling constant α . The numerical code uses a standard C-grid, second order spatial discretization and a leap-frog time integrator corrected by a Robert-Asselin filter. We use the

initial condition $u = v = 0$ and $h' = A \sin(\pi x/L) \sin(\pi y/L)$, with $A = 10^{-3}m$.

For the particular case of $\alpha = 5 \times 10^{-6} m s^{-2}$ we have performed integrations 500 years long. This allows the system to reach an equilibrium in which the nonlinear terms arrest the initial exponential growth. Figure 3 shows four snapshots of h' which span 2.2 years in the equilibrated regime. The similarity with the damped, uncoupled mode of figure 2 is evident. Some subtle effects of nonlinearity are revealed upon inspection of the available potential energy, whose time evolution is plotted in Figure 4. The inset shows 30 years within the equilibrated regime. In the growing regime the oscillations have a period of 4.4 years, in agreement with the linear theory (because the available potential energy is a quadratic quantity it oscillates at half the period). In the equilibrated regime period doubling emerges, characterized by an alternance of high and low maxima. Thus, the period of the nonlinear system is 8.8 years.

Period doubling bifurcations are common in nonlinear dynamical systems with quadratic nonlinearities. Here the most important nonlinearity is the mass flux divergence $\nabla h' \mathbf{u}$. In this regime, this quadratic term is more important than advection of momentum, as demonstrated by numerical solutions of (1) without advection of momentum. The result (not shown here) is that, for $\alpha = 5 \times 10^{-6} m s^{-2}$, the available potential energy oscillates with an amplitude which is 9% greater than in the case of the full equations and there is no appreciable difference in the period.

The onset of subharmonic frequencies is also reported by S00 in simulations which, in addition to the wind-coupling (2), include spatially inhomogeneous stochastic forcing. S00 interpret this phenomenon in terms of a spatial resonance between Rossby waves and small-scale Reynolds fluxes of momentum that are stochastically induced. Our results suggest that the *linear* excitation of a basin-scale oceanic mode

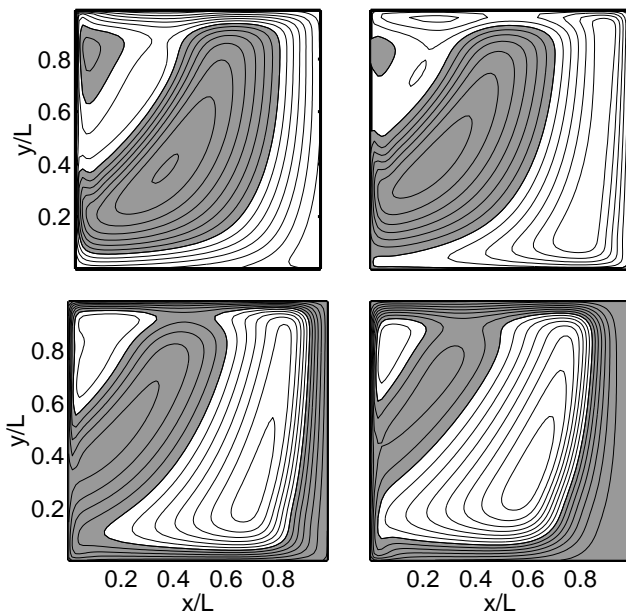


Figure 3. Four snapshots of h' solution of (1), every 0.55 years. The coupling constant is $\alpha = 5 \times 10^{-6} m s^{-2}$. The other parameters are given in Table 1. The contour interval is 20 m and negative values are shaded.

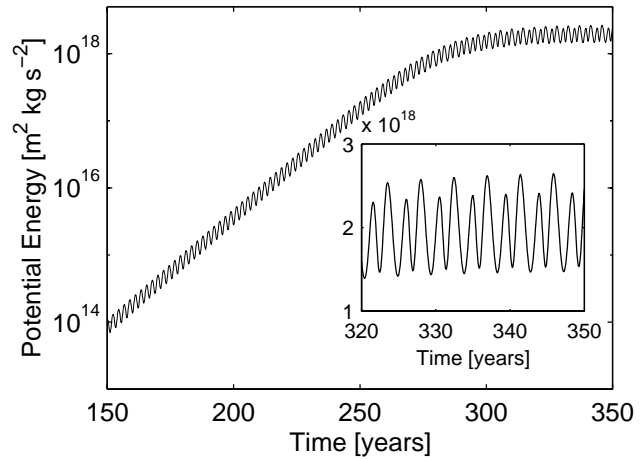


Figure 4. Available potential energy versus time for the numerical solution of (1). The inset evidences the period doubling. The coupling constant is $\alpha = 5 \times 10^{-6} m s^{-2}$. The other parameters are given in Table 1.

by air-sea coupling leads to similar low frequency variability, which then undergoes period-doubling due to mass-flux nonlinearities.

Discussion

The reduced-gravity shallow water equations in a closed basin exhibit damped basin modes. The air-sea coupling merely allows these modes to overcome the damping effect of friction, and to become sustained.

The oscillation in figure 2 and figure 3 can be heuristically described as an interaction between long Rossby waves impinging upon the western boundary and a basin-wide displacement of the coastal-height level. The latter is necessary in order to conserve mass. The arrival of the maximum height displacement at the western boundary (located at $y \approx 0.3L$ in figure 3) induces a large nonlocal readjustment which triggers a new Rossby wavefront from the eastern wall. This is why the linear period coincides with the long Rossby wave transit time (7) at that latitude.

In the conventional calculation of linear quasigeostrophic basin modes reported in [Pedlosky, 1987] the pressure, proportional to h' , is set to zero along the boundaries, and the basin modes documented here are suppressed. However, [McWilliams, 1977] shows that mass conservation requires the boundary pressure to be an unknown function of time, subject to the constraint that the basin-wide average of h' vanishes. This boundary condition enables the quasigeostrophic analogue of our basin modes [Cessi and Primeau, 2001].

The mode of oscillation documented here is distinct from that arising through a delayed feedback mechanism. In the calculations discussed by [Jin, 1997; Munich et al., 1998; GC00] the ocean-only mode of variability is suppressed by the eastern boundary condition of zero pressure anomaly, i.e. $h' = 0$ at $x = L$.

The existence of large scales basin modes rely on two simple physical principles, namely mass conservation and planetary geostrophy. These are general constraints which should guarantee that the phenomenology we described is fairly robust. Further work will be needed to assess the properties

of these basin modes in geometries with realistic coastlines and with more sophisticated coupling to the atmosphere.

Acknowledgments. Funding is provided by the National Science Foundation and the Department of Energy.

References

- Battisti, D.S. and U.S. Bhatt and M.A. Alexander, A modeling study of the interannual variability in the wintertime North Atlantic Ocean, *J. Climate*, *8*, 3067-3083, 1995.
- Berloff, P. and S. Meacham, The dynamics of an equivalent-barotropic model of the wind-driven circulation, *J. Mar. Res.*, *55*, 407-451, 1997.
- Bjerknes, J., Atlantic air-sea interaction, *Adv. Geophysics* *10*, 1-82, 1964.
- Cessi, P. and S. Louazel, Decadal oceanic response to stochastic wind forcing *J. Phys. Oceanogr.*, *In press*, 2001.
- Cessi, P. and F. Primeau, Dissipative selection of low-frequency modes in a reduced-gravity basin *J. Phys. Oceanogr.*, *31*, 127-137, 2001.
- Curry, R.G. and M.S. McCartney and T.M. Joyce, Oceanic transport of subpolar climate signals to mid-depth subtropical waters, *Nature*, *391*, 575-577, 1998.
- Gallego, B. and P. Cessi, Exchange of heat and momentum between the atmosphere and the ocean: a minimal model of decadal oscillations, *Climate Dyn.*, *16*, 479-489, 2000.
- Jin, F.F., A theory of interdecadal climate variability of the North Pacific ocean-atmosphere system, *J. Climate*, *10*, 1821-1835, 1997.
- Latif, M., Dynamics of interdecadal variability in coupled ocean-atmosphere models, *J. Climate*, *11*, 602-624, 1998.
- McWilliams, J.C., A note on a consistent quasigeostrophic model in a multiply connected domain. *Dyn. Atmos. Oceans.*, *1*, 427-441, 1977.
- Munich, M. and M. Latif and S. Venzke and E. Maier-Reimer, Decadal oscillations in a simple coupled model, *J. Climate*, *11*, 3309-3319, 1998.
- Nakamura, H. and G. Lin and T. Yamagata, Decadal climate variability in the North Pacific, *Bull. Amer. Meteor. Soc.*, *78*, 2215-2225, 1997.
- Pedlosky, J. *Geophysical fluid dynamics*. 710 + xiv pp., Springer-Verlag, 1987.
- Rogers, J.C., North Atlantic storm track variability and its association to the North Atlantic oscillation and climate variability of northern Europe, *J. Climate*, *10*, 1635-1647, 1997.
- Sura, P. and F. Lunkett and K. Fraedrich, Decadal variability in a simplified wind-driven ocean model, *J. Phys. Oceanogr.*, *30*, 1917-1930, 2000.
- Ting, M. and H. Wang, Summertime US precipitation variability and its relation to Pacific sea surface temperature, *J. Climate*, *10*, 1853-1873, 1997.
- Trenberth, K.E. and J.W. Hurrell, Decadal atmosphere-ocean variations in the Pacific, *Climate Dyn.*, *9*, 303-319, 1994.

P. Cessi and F. Paparella, Scripps Institution of Oceanography, UCSD-0213, La Jolla, CA 92093-0213. (e-mail: pcessi@ucsd.edu, francesco.paparella@unile.it)

(Received November 17, 2000; accepted March 22, 2001.)